










## Observation of a positive-parity wave in the low-energy spectrum of ${}^7\text{He}$

M. S. Golovkov <sup>1</sup>, A. A. Bezbakh <sup>1,2,\*</sup>, A. S. Denikin <sup>1,2</sup>, R. Wolski <sup>1</sup>, S. G. Belogurov,<sup>1,3</sup> D. Biare,<sup>1</sup> V. Chudoba,<sup>1,4</sup> E. M. Gazeeva,<sup>1</sup> A. V. Gorshkov,<sup>1</sup> G. Kaminski <sup>1,5</sup>, B. R. Khamidullin <sup>1,6</sup>, S. A. Krupko,<sup>1</sup> B. Mauey,<sup>1,7</sup> I. A. Muzalevskii <sup>1,4</sup>, W. Piatek,<sup>1,5</sup> A. M. Quynh <sup>1,8</sup>, R. S. Slepnev,<sup>1</sup> A. Swiercz,<sup>1</sup> P. Szymkiewicz,<sup>1</sup> and B. Zalewski <sup>1,5</sup>

<sup>1</sup>Flerov Laboratory of Nuclear Reactions, JINR, 141980 Dubna, Russia

<sup>2</sup>Department of Nuclear Physics, Dubna State University, 141982 Dubna, Russia

<sup>3</sup>Institute of Nuclear Physics and Engineering, National Research Nuclear University “MEPhI”, 115409 Moscow, Russia

<sup>4</sup>Institute of Physics, Silesian University in Opava, 74601 Opava, Czech Republic

<sup>5</sup>Heavy Ion Laboratory, University of Warsaw, 02-093 Warsaw, Poland

<sup>6</sup>Department of Nuclear-Physical Materials Science, Kazan Federal University, 420111 Kazan, Russia

<sup>7</sup>Faculty of Physics and Technology, L. N. Gumilyov Eurasian National University, 010008 Astana, Kazakhstan

<sup>8</sup>Nuclear Research Institute, 670000 Dalat, Vietnam



(Received 5 February 2024; revised 4 April 2024; accepted 16 May 2024; published 14 June 2024)

The  ${}^7\text{He}$  nucleus was studied by the  $(d, p)$  reaction at 29A MeV beam energy. The  ${}^7\text{He}$  spectrum was measured up to 8 MeV above the  ${}^6\text{He}+n$  threshold. The forward-backward asymmetry in the neutron emission from unbound states of  ${}^7\text{He}$  has been found. That implies the presence of a positive parity partial wave in the  ${}^7\text{He}$  spectrum.

DOI: [10.1103/PhysRevC.109.L061602](https://doi.org/10.1103/PhysRevC.109.L061602)

**Introduction.** For a long time after the first observation of the  ${}^7\text{He}$  helium isotope in the  ${}^7\text{Li}(t, {}^3\text{He}){}^7\text{He}$  charge exchange reaction [1], it was assumed that, like  $A = 3$  nuclei,  ${}^7\text{He}$  has no excited states. The excited state of  ${}^7\text{He}$  ( $E^* = 2.9 \pm 0.3$  MeV,  $\Gamma = 2.2 \pm 0.3$  MeV) was observed for the first time in the one-neutron transfer reaction  $p({}^8\text{He}, d){}^7\text{He}$  [2]. This was followed by a series of experimental works in which the spectrum of excited states of  ${}^7\text{He}$  was studied in various reactions [3–9]. A review of both theoretical calculations and experimental results for the  ${}^7\text{He}$  excitation spectrum can be found in Ref. [9]. Most of the model calculations predict the sequence  $J^\pi = 1/2^-, 5/2^-, 3/2^-$  for the first three excited states lying at 2 to 3 MeV above the ground state  $J^\pi = 3/2^-$ , but the experimental results demonstrate a significant dispersion. However, if one restricts the analysis to works where one-nucleon transfer reactions were used to populate the excited states of  ${}^7\text{He}$  then the experimental data generally agree with the model predictions. In the case of the deuteron stripping reaction, when the  ${}^7\text{He}$  nucleus is produced due to the neutron transfer to  ${}^6\text{He}$ , apart from the ground state, the resonance at an energy of 2.6 MeV with a width of  $\approx 2$  MeV, is populated [6]. This state predominantly decays through the channel  ${}^7\text{He}^* \rightarrow n + {}^6\text{He}(\text{gs})$ , however; there is a noticeable decay branch leading to the first excited state of  ${}^6\text{He}$  (1.8 MeV,  $2^+$ ). In the neutron pickup  ${}^8\text{He}(d, p)$  [2] or the proton pickup reaction  ${}^8\text{Li}(d, {}^3\text{He})$  [9], a broad state at an excitation energy of  $\approx 3$  MeV decaying exclusively through the  ${}^7\text{He}^* \rightarrow n + {}^6\text{He}(2^+)$  channel is observed. The analysis of spectroscopic factors and angular distributions within the distorted-wave Born approximation (DWBA) framework led

the authors of [9] to propose a sequence of  ${}^7\text{He}$  nucleus negative parity states  $J^\pi = 3/2^-, 1/2^-, 5/2^-$ . It should be noted that until now no experimental evidence of positive-parity states in the spectrum has been reported, although there are theoretical indications of such a possibility. It is well known that the nuclear shell structure breaks down with distance from the stability line. For example, for isotopes of Be, as the neutron excess increases, inversion of the  $1p_{1/2}$  and  $2s_{1/2}$  shells occurs. However, the expected significant width of the  $s_{1/2}$  resonance, due to the absence of barrier factors, makes it problematic to identify this state in the continuum. Till now, information about the structure of the spectrum of excited states of the  ${}^7\text{He}$  nucleus has been based on the analysis of the missing (or invariant) mass spectra for various reactions, in some cases supplemented by the identification of the decay channel. One of the possible methods for determining the spins and parities of the states lying above the decay threshold can be the measurement of the angular distributions of the decay products if the reaction mechanism leading to the population of the corresponding states is known.

**Experiment.** Measurements of the  ${}^2\text{H}({}^6\text{He}, p)$  reaction leading to population of the low energy  ${}^7\text{He}$  spectrum were performed at the beginning of 2020 at the ACCULINNA-2 facility at U-400M heavy-ion cyclotron, Flerov Laboratory of Nuclear Reaction (JINR, Dubna) [10]. First results of the analysis, concentrating on the properties of the  ${}^7\text{He}$  ground state and a detailed description of the experimental setup, were reported in [11]. Here we extend the analysis of the experimental data related with decay properties of the  ${}^7\text{He}$  excited states. A secondary  ${}^6\text{He}$  beam at 29A MeV (with  $\approx 95\%$  purity) was produced via the fragmentation of the primary  ${}^{11}\text{B}$  beam on 1 mm thick beryllium target. After cleaning, the  ${}^6\text{He}$  beam bombarded a target filled with deuterium at a

\*Contact author: bezbakh@jinr.ru

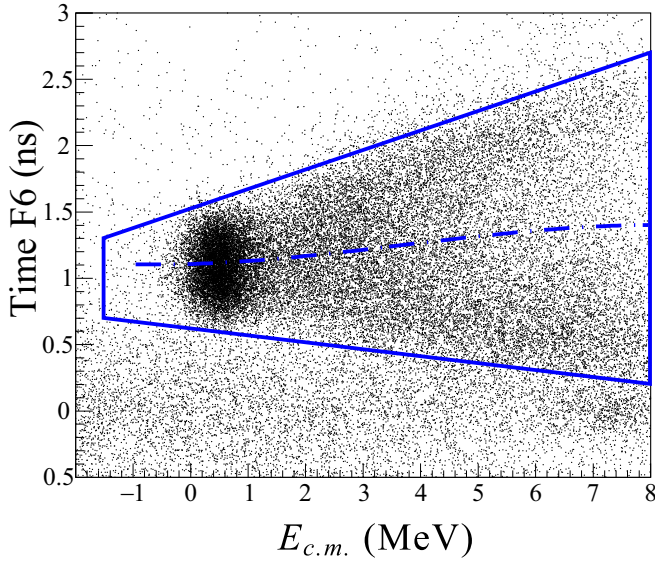


FIG. 1. Missing mass spectrum of the  ${}^7\text{He}$  from the  ${}^2\text{H}({}^6\text{He}, p){}^7\text{He}$  reaction versus time of flight of the  ${}^7\text{He}$  decay product from the target to the F6 detector. The missing mass spectrum was obtained based on the registration of the recoil proton in coincidence with  ${}^4\text{He}$  or  ${}^6\text{He}$  which hit the F6 detector. See text for the details.

temperature of 26 K and a pressure of 1.48 atm. The particle beam energy was measured using a standard time-of-flight (ToF) technique with fast plastic scintillators. Two multiwire proportional chambers installed upstream of the target at a distance of 270 and 814 mm were used to determine the trajectories of the incident  ${}^6\text{He}$  particles and their coordinates in the target plane.

The energies and the angles of the backward recoiled protons were measured with an array of four telescopes located upstream of the target at a distance of 134 mm and subtended the angular range of  $\approx 150^\circ$ – $170^\circ$  relative to the beam direction. Each telescope consisted of two square silicon detectors  $64 \times 64 \text{ mm}^2$  in size and 1 mm thick. Double-sided detectors (DSDs), mounted closer to the target, had  $32 \times 32$  strips and provided measurements of the energy and position of the proton. The second single sided detector (SSD) was used as a veto detector.

Another plastic scintillator (EJ-212) 100 mm in diameter and 250  $\mu\text{m}$  thick (F6 detector) was installed on the beam axis at a distance of 83 cm downstream from the target.

The registration of neutrons was performed using an array of detectors with 48 modules based on stilbene crystals [12] with a low threshold for  $n$ - $\gamma$  discrimination. The detector array was installed behind the reaction chamber at a distance of 3 m from the target. The neutron energy was measured by the ToF method. Observation of the  $\gamma$ -peak with 0.6 ns (FWHM) width from the interaction of the beam with target provide the absolute calibration and the accuracy of neutron energy measurements.

**Measurement results.** Figure 1 shows a two-dimensional distribution of events corresponding to the coincidence registration of protons from the reaction  ${}^2\text{H}({}^6\text{He}, p){}^7\text{He}$  with charged decay products  ${}^7\text{He} \rightarrow {}^6\text{He}(0^+) + n$  or  ${}^7\text{He} \rightarrow$

${}^6\text{He}(2^+) + n \rightarrow \alpha + 3n$  which hit the F6 detector. The abscissa is the  ${}^7\text{He}$  excitation energy above the  ${}^7\text{He} \rightarrow {}^6\text{He} + n$  energy threshold. The ordinate shows the time F6, which is a difference between the measured ToF of decay particles ( ${}^6\text{He}$  or  $\alpha$ ) from the target to the detector F6 and the calculated ToF of the beam ions on the same ToF base. This quantity is proportional to the detectable particle longitudinal momentum. The trapezoidal area marked in Fig. 1 with the solid line confines the range of time F6 values for the events from the  ${}^7\text{He}$  decay and clearly demonstrates an increase in the longitudinal momentum range appearing with the increase of the  ${}^7\text{He}$  excitation energy. Events lying outside this structure correspond to the background generated mainly by the random coincidences of protons with the products of the beam interaction with the material of the target windows.

Assuming a pole mechanism for the reaction  ${}^2\text{H}({}^6\text{He}, p){}^7\text{He}$ , the angular distribution of the  ${}^7\text{He} \rightarrow {}^6\text{He} + n$  decay must have axial symmetry with respect to the direction of the momentum  $\mathbf{q}$  transferred in the reaction:  $\mathbf{q} = \frac{m_{{}^6\text{He}}}{m_{{}^7\text{He}}} \mathbf{k}_{{}^7\text{He}} - \mathbf{k}_{{}^6\text{He}}$ , where  $\mathbf{k}_{{}^6\text{He}}$  and  $\mathbf{k}_{{}^7\text{He}}$  are the corresponding momenta in the center-of-mass frame of the reaction. The registration of protons at small angles ensures that the direction of the transferred momentum  $\mathbf{q}$  is close to the beam axis, which, in turn, leads to a strong correlation of the measured time F6 with the direction (forward-backward) of the emission of helium nuclei relative to  $\mathbf{q}$  in the  ${}^7\text{He}$  center-of-mass system. To estimate the correlation between direction of the helium emission and measured time F6 we perform Monte Carlo calculation by using the GEANT4 software package [13] with condition that  ${}^7\text{He} \rightarrow {}^6\text{He} + n$  decays at an angle of  $\pi/2$  with respect to the direction of the transferred momentum  $\mathbf{q}$ . The dashed line in Fig. 1 shows the most probable time F6 under this condition. The ToF difference between forward and backward decay events decreased with decreasing excitation energy and became comparable with time resolution in the region of the ground state peak. Due to registration coincidences with neutrons we have alternative, completely independent way to estimate angular asymmetry for energies below 1 MeV. Neutron measurements confirm that, even for an energy of 0.4 MeV, the time F6 remains sensitive to angular asymmetry (see the Discussion section below).

In Fig. 2, the thin line shows the missing mass spectrum of  ${}^7\text{He}$  corresponding to the events in the selected area of the two-dimensional plot with background subtraction. The background estimation is based on measurements with an empty target normalized to the same beam flux integral. The spectrum is dominated by the peak corresponding to the population of the  ${}^7\text{He}$  nucleus in its ground state ( $J^\pi = 3/2^-$ ). The peak width ( $\approx 600 \text{ keV}$ , FWHM) noticeably exceeds the intrinsic  ${}^7\text{He}$  ground state width and demonstrates the experimental resolution, which is mainly determined by the target thickness and energy losses of protons with relatively low energy (2–5 MeV). The filled histogram and thick line show the spectra corresponding to events lying above and below the dashed line in Fig. 1, respectively.

If the spectrum was formed exclusively by  $p$ -wave resonances (known from literature data), we should observe

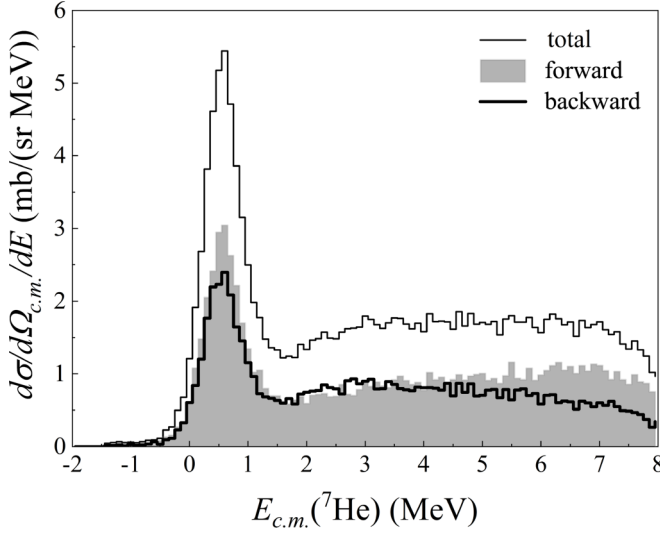


FIG. 2. Experimental missing mass spectrum of  ${}^7\text{He}$  obtained for events limited by the trapezoidal contour shown in Fig. 1 and is shown by the thin line. The filled histogram and thick line show the spectra corresponding to events lying below and above the dashed line in Fig. 1, respectively. All spectra are presented with background subtracted.

a symmetric picture. However, even for the peak of the ground state of  ${}^7\text{He}$  clear asymmetry of the decay products with respect to the direction of the transferred momentum is observed.

The observed asymmetry indicates the presence of a wave of opposite parity; the natural assumption (due to the proximity of the threshold and barrier factors) allows us to associate the observed asymmetry with the manifestation of  $s$ - $p$  interference.

It was noted in [14] that the cross section of the stripping reaction leading to the population of states in the continuum (quasibound resonances) is determined, to a large extent, by the behavior of the total cross section of the interaction of the transferred particle with the target nucleus. Experimental evidence of this connection was demonstrated in [15] by comparing the total neutron scattering cross section for the  ${}^{15}\text{N}$  nucleus with the proton spectra from the  ${}^{15}\text{N}(d, p){}^{16}\text{N}(\text{unbound})$  reaction.

It is shown that the spectra of protons from the transfer reaction are reproduced (with appropriate corrections) by the resonant structure of the neutron scattering excitation function, including the effects of interference of narrow resonances with a smooth background from potential scattering.

Following [16], in the plane-wave approximation, the partial differential cross section of the  $(d, p)$  reaction in the vicinity of an isolated resonance can be expressed in terms of the total cross section for the interaction of virtual neutron with a target outside the energy shell  $\sigma_l^{(\text{tot,off})}(p_n, E_n)$ :

$$\left(\frac{d^3\sigma}{d\Omega_p dE_p}\right)_l = \frac{2m^2}{(2\pi\hbar)^3} \frac{p_p}{p_d} \frac{|M_{d,pn}|^2}{\left[\frac{1}{m}\left(\frac{1}{2}p_d - p_p\right)^2 + \epsilon_d\right]^2} \frac{p_n}{m} \sigma_l^{(\text{tot,off})}(p_n, E_n),$$

TABLE I.  $R$ -matrix parameters. The channel radius was taken to be 4.5 fm.

	$J^\pi$	$E$ (MeV)	$\Gamma$ (MeV)
$1p$	$3/2^-$	0.38	0.11
$2s$	$1/2^+$	2.0	2.0
$1p$	$1/2^-$	2.4	2.0

where  $p_n$  is the virtual neutron momentum and  $E_n$  is the relative energy in the neutron-target subsystem in the exit channel.

The optical theorem provides the relation between the total reaction cross sections on and off the energy shell in the following form:

$$p_n \sigma_l^{(\text{tot,off})}(p_n, E_n) = \left[ \frac{M_l^2(p_n)}{M_l^2(k_n)} \right] k_n \sigma_l^{(\text{tot,on})}(E_n),$$

where  $k_n = \sqrt{2\mu E_n}$ , and the amplitude ratio  $M_l$  (following [15]) can be defined as the ratio of the penetrability factors defined within the  $R$ -matrix theory. Unlike previous works that analyzed only the missing mass spectra, our experiment also detected decay products of  ${}^7\text{He}$  resonances in addition to protons from the  ${}^2\text{H}({}^6\text{He}, p){}^7\text{He}$  reaction. Therefore, we represented the cross section of the process through the square of the coherent sum of partial amplitudes, taking into account corrections related to departure from the energy surface as recommended in [16]:

$$f_l^{(\text{off})}(p_n, E_n) = \sqrt{\frac{k_n}{p_n} \frac{M_l(p_n)}{M_l(k_n)}} f_l^{(\text{on})}(E_n).$$

The applicability of this approximation was tested on a simple potential model with the potential reproducing a narrow resonance in  $p$  wave, and was found to be satisfactory for the energies under the interest. Distorted-wave effects were counted by means of weakly bound state DWBA calculations.

Having in mind the available experimental data, we limited ourselves to taking into account three partial amplitudes:  $s_{1/2}$ ,  $p_{1/2}$ , and  $p_{3/2}$ . To calculate the phase shifts and amplitudes on the energy shell we used the program AZURE2 [17] with the parameters given in Table I. Resonance parameters for the  ${}^7\text{He}$  ground state were taken from the fit of experimental data (see Ref. [11]). The impact of the experimental setup efficiency was simulated by using the GEANT4 software package [13].

Figure 3 shows the results of model calculations, taking into account instrumental resolution, in a format similar to the experimental data presented in Fig. 2. In Fig. 3(a) calculations are shown where only  $p$ -wave resonances known from the literature are included as initial parameters, i.e.,  $1p_{3/2^-}$  and  $1p_{1/2^-}$  resonances listed in Table I. As expected, the calculation gives an almost symmetric forward-to-backward distribution with respect to the direction of the momentum transferred in the reaction. In addition to the  $p$ -wave resonances, nonresonant  $s$  scattering (scattering on an opaque sphere) was added to obtain the observed asymmetry for the ground state peak. But interference of nonresonant  $s$  wave with higher-laying negative parity states inevitably leads to

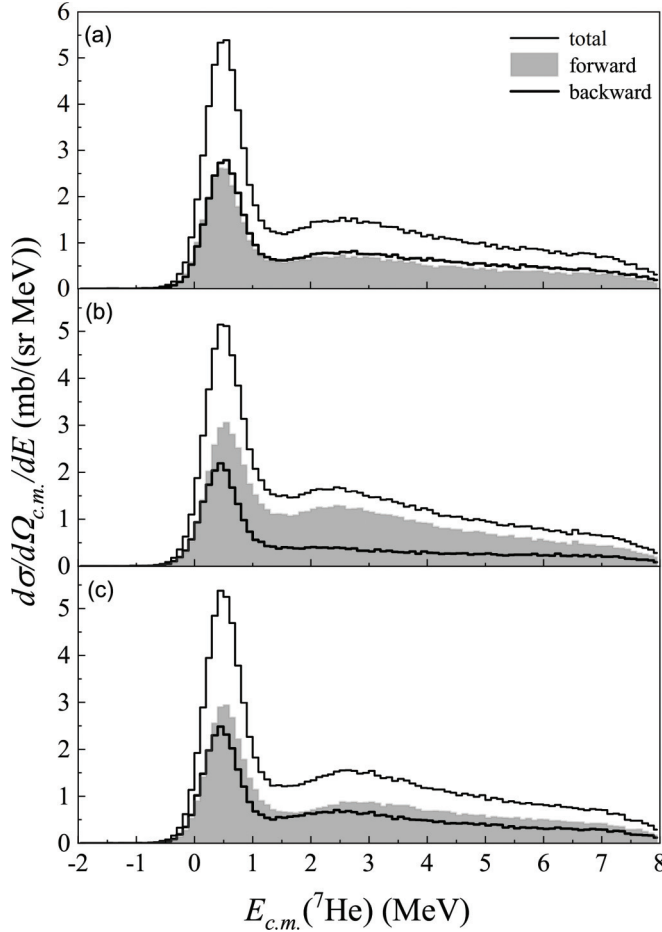


FIG. 3. Calculated missing mass spectrum of the  ${}^7\text{He}$  in the same format as in Fig. 2. (a) Only  $p$ -wave resonances were included in the model, (b)  $p$ -wave resonances plus nonresonant (hard-sphere scattering)  $s$  wave, (c) the same plus broad  $s$ -wave resonance was included. The  $R$ -matrix parameters are presented in Table I.

strong asymmetry above 1.5 MeV, as shown in Fig. 3(b). The only way to suppress this asymmetry is to introduce the broad  $s$ -wave resonant state at about 2 MeV. The results of the model calculation with broad  $s$ -wave state are shown in Fig. 3(c). When comparing the calculation in Fig. 3(c) with the experimental spectrum in Fig. 2, it should be kept in mind that the calculated spectrum takes into account only the elastic decay channel  ${}^7\text{He} \rightarrow {}^6\text{He}(0^+) + n$ , while the experimental data unambiguously indicate the presence of the  ${}^7\text{He} \rightarrow {}^6\text{He}(2^+) + n$  decay channel at energy greater than 2 MeV, and the products of  ${}^7\text{He}$  decay through the excited state fly out in the laboratory coordinate system in a narrower cone, providing a higher detection efficiency and, thus, an additional increase in the count in the experimental spectrum compared to the model one. An additional contribution to the rise in the experimental cross section can also be made by high-lying resonances not included in the model analysis. Figure 4 shows the behavior of the  $s_{1/2}$ ,  $p_{1/2}$ , and  $p_{3/2}$  phase shifts of the partial waves included in the model calculation.

Coincidences with neutrons from the decay of  ${}^7\text{He}$  were also detected in the present experiment. The neutron

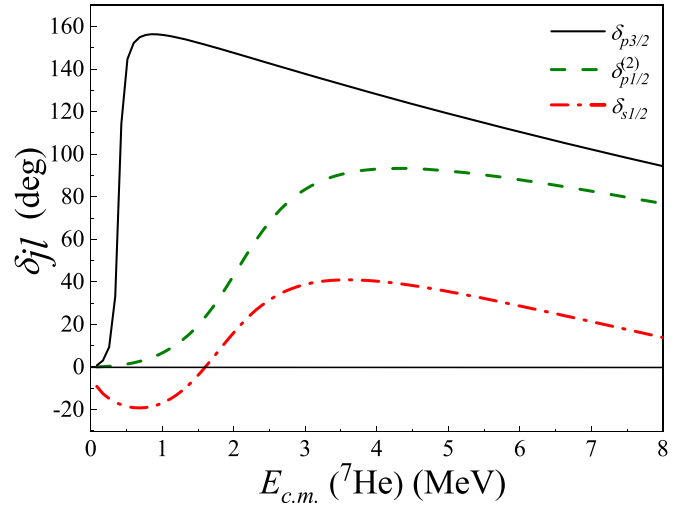


FIG. 4. Phase shifts for the partial waves calculated using AZURE2 code with the parameters listed in Table I, showing the behavior of the  $p_{3/2}$ ,  $p_{1/2}$ , and  $s_{1/2}$  phase-shifts of the partial waves included in the model calculation, as the black line, green dotted line, and red dash-dotted line, respectively.

detector covers the angles up to  $20^\circ$  in the laboratory system, which corresponds to the limiting neutron emission angles in the decay of  ${}^7\text{He}$  with an excitation energy of  $\approx 1.5$  MeV. At higher excitation energies, the neutron emission cone in the laboratory system exceeds the angular acceptance of the detector, and the efficiency of detecting coincidences with neutrons drops sharply. But even in the region of full angular acceptance, the neutron detection efficiency is on the order of several percent. Nevertheless, the registration of neutrons (which corresponds to the conditions of a complete kinematic experiment) makes it possible to significantly improve the instrumental resolution and restore the angular distribution of the decay products with good accuracy.

Figure 5 shows the excitation energy spectrum of  ${}^7\text{He}$  for coincidences of protons,  ${}^6\text{He}$ , and neutrons from the reaction  ${}^2\text{H}({}^6\text{He}, p){}^7\text{He} \rightarrow {}^6\text{He} + n$ . The experimental data are shown as points with statistical errors; the histogram is a model calculation with the parameters given in Table I. The effect of the experimental setup was estimated by the Monte Carlo method using the GEANT4 software package; the instrumental resolution was estimated to be  $\approx 140$  keV (FWHM), a value comparable to the resonance intrinsic width.

Figure 6 presents the neutron angular distribution from the  $(3/2^-) \rightarrow {}^6\text{He} + n$  decay in the  ${}^7\text{He}$  center-of-mass system with respect to the direction of the transferred momentum in the reaction. Neutron measurements provide an alternative way to estimate the angular asymmetry in the region of the ground state peak counts( $\theta < 90^\circ$ )/counts( $\theta > 90^\circ$ ) = 1.25(25). Only statistical errors are taken. This coincides with a value 1.23 obtained from the measurement of time F6 in the region 0–1 MeV (Fig. 2). The filled histogram displays the result of model calculations with the parameters given in Table I, and the histogram represented by a line corresponds to a calculation in which only the  $p$  wave is present

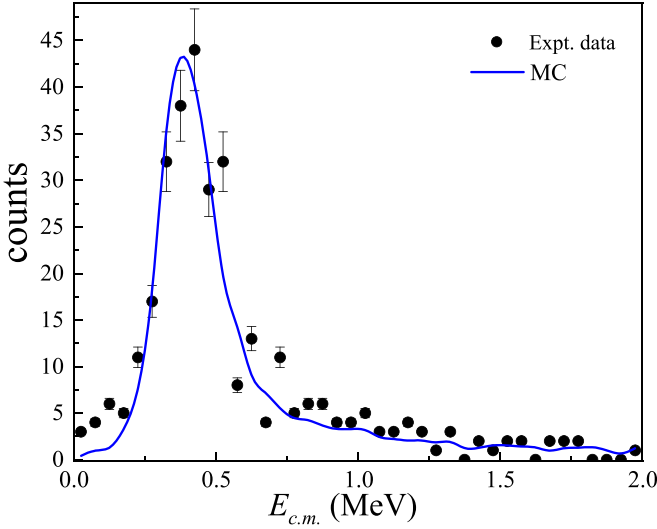


FIG. 5. The  ${}^7\text{He}$  excitation energy spectrum obtained for the reaction channel  ${}^2\text{H}({}^6\text{He}, p){}^7\text{He} \rightarrow {}^6\text{He}(\text{gs}) + n$ . The spectrum is reconstructed from the proton-neutron coincidence events (filled circles with error bar). The solid line is the result of MC calculations with  $R$ -matrix parameters  $E_{\text{res}} = 0.38$  MeV and  $\Gamma_{\text{res}} = 0.11$  MeV for the  ${}^7\text{He}$  ground-state resonance.

(symmetric distribution). The corresponding  $\chi$ -square values for calculations with (without)  $s$  wave are 0.9 (1.1).

**Discussion and conclusions.** The excitation spectrum of  ${}^7\text{He}$  was measured in the range 0–7 MeV in the reaction  ${}^2\text{H}({}^6\text{He}, p)$ . The measurement of the time of flight of the decay products of  ${}^7\text{He}$  made it possible to reveal the asymmetry of the angular distribution with respect to the direction of the momentum transferred in the reaction. Within the framework of the pole mechanism of the reaction  ${}^6\text{He}(d, p){}^7\text{He}$ , this indicates the interference of the waves of different parity during the formation of a continuous spectrum.

The analysis of experimental data was carried out on the basis of the Shapiro dispersion theory. Within this model, the observed asymmetry of the angular distribution may be explained by the presence of a broad  $s$  state at the energy of  $\approx 2$  MeV above the neutron decay threshold. The corresponding phase shifts are shown in Fig. 4. The spectrum is formed by the three resonance structures:  $3/2^-$  (gs),  $1/2^-$ , and  $1/2^+$ . The parameters of the ground state and its spin partner ( $1/2^-$ ) generally agree with the observations made in previous papers [6], while the  $2s_{1/2}$  state is observed for the first time. The discrepancy between model calculations and experiment for  ${}^7\text{He}$  excitation energies above 3 MeV is due to the fact that the model takes into account only one decay channel  ${}^7\text{He} \rightarrow {}^6\text{He}(0^+) + n$ , while the experimental data indicate a significant contribution from the  ${}^7\text{He} \rightarrow {}^6\text{He}(2^+) + n$  decay channels. In addition, the rise in the cross section at high energies can be associated with the population of higher-lying states. The detection of neutrons made it possible to obtain a record resolution in the spectrum of the missing mass of  ${}^7\text{He}$ ,

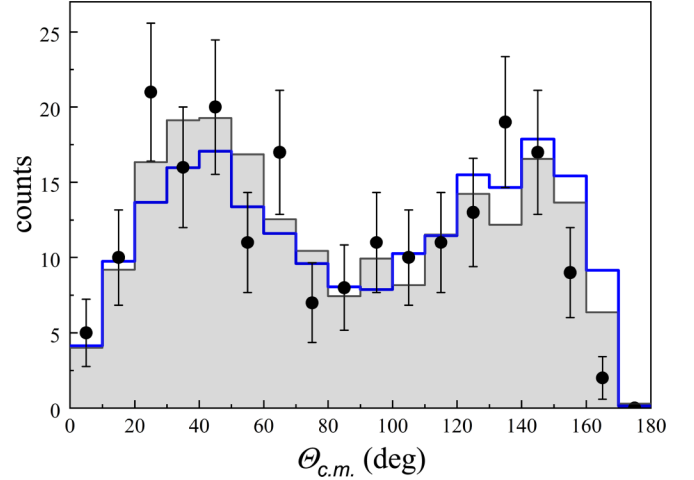


FIG. 6. Neutron angular distribution  $d\sigma/d\theta$  from the decay of the  ${}^7\text{He}$  ground state. Filled circles with error bar are experimental data, the filled histogram is a model calculation with the parameters given in Table I, and calculations without  $s$  wave are shown by the blue histogram.

comparable to the intrinsic width of the  ${}^7\text{He}$  ground state. As a result, our estimation of the  ${}^7\text{He}$  ground state width gives us  $\Gamma = 0.11$  MeV, which is rather less in comparison with previous results ( $\Gamma = 0.182(5)$  [18] or  $\Gamma = 0.14$  MeV [19]). It should be noted that neutron detection in our experiment provides the best instrumental resolution and hence the minimal impact of the setup on intrinsic width evaluation. Besides, the measured ground state angular distribution provides additional confirmation of the angular asymmetry observation.

In the most theoretical work [20–22] the  $s$  phase is characterized by a monotone decrease from the threshold and only one *ab initio* calculation [23] predicts the  $s$ -wave resonant behavior with parameters close to our findings. Our results should be of more interest since they raise the question of shell inversion in the He isotope. That is a challenge both for the theoretical calculations and for the applicability of the presented way of experimental data analysis. Our treatment is based on the observation of angular asymmetry of the  ${}^7\text{He}$  decay and can be considered as an indication of the presence of a broad  $s$  resonance above  ${}^7\text{He} \rightarrow {}^6\text{He} + n$  threshold. Obviously, precise measurement of the angular distribution of the  ${}^7\text{He}$  decay in a wide range of excitation energy would provide a reliable basis for proving the applicability transfer reaction as a source of unique information about the nuclear structure.

**Acknowledgments.** This work was partly supported by the Russian Science Foundation Grant No. 22-12-00054 and in the frame of theme No. 6 “Nuclear and radiation physics” of NCPHM, topic “Simulation experiments, developing experimental methods and theory development in nuclear reactions with heavy ions at low and intermediate energies.” We are grateful to Prof. Yu M. Tchuvil’sky for fruitful discussion and Prof. S. I. Sidorchuk for the interest and support of this activity.

- [1] R. H. Stokes and P. G. Young, New isotope of helium:  $^7\text{He}$ , *Phys. Rev. Lett.* **18**, 611 (1967).
- [2] A. A. Korshennikov, M. S. Golovkov, A. Ozawa, E. A. Kuzmin, E. Y. Nikolskii, K. Yoshida, B. G. Novatskii, A. A. Ogloblin, I. Tanihata, Z. Fulop, K. Kusaka, K. Morimoto, H. Otsu, H. Petrascu, and F. Tokanai, Observation of an excited state in  $^7\text{He}$  with unusual structure, *Phys. Rev. Lett.* **82**, 3581 (1999).
- [3] M. S. Golovkov, I. Tanihata, D. D. Bogdanov, M. L. Chelnokov, A. S. Fomichev, V. A. Gorshkov, Y. T. Oganessian, A. M. Rodin, S. I. Sidorchuk, S. V. Stepantsov, G. M. Ter-Akopian, R. Wolski, W. Mittig, P. Roussel-Chomaz, H. Savajols, E. A. Kuzmin, E. Y. Nikolskii, B. G. Novatskii, and A. A. Ogloblin, Spectroscopy of  $^7\text{He}$  and superheavy hydrogen isotope  $^5\text{H}$ , *Phys. At. Nucl.* **64**, 1244 (2001).
- [4] H. G. Bohlen, R. Kalpakchieva, A. Blažević, B. Gebauer, T. N. Massey, W. von Oertzen, and S. Thummerer, Spectroscopy of  $^7\text{He}$  states using the ( $^{15}\text{N}$ ,  $^{17}\text{F}$ ) reaction on  $^9\text{Be}$ , *Phys. Rev. C* **64**, 024312 (2001).
- [5] M. Meister, K. Markenroth, D. Aleksandrov, T. Aumann, L. Axelsson, T. Baumann, M. J. G. Borge, L. V. Chulkov, W. Dostal, B. Eberlein, T. W. Elze, H. Emling, C. Forssén, H. Geissel, M. Hellström, R. Holzmann, B. Jonson, J. V. Kratz, R. Kulesa, Y. Leifels *et al.*, Evidence for a new low-lying resonance state in  $^7\text{He}$ , *Phys. Rev. Lett.* **88**, 102501 (2002).
- [6] A. H. Wuosmaa, K. E. Rehm, J. P. Greene, D. J. Henderson, R. V. F. Janssens, C. L. Jiang, L. Jisonna, E. F. Moore, R. C. Pardo, M. Paul, D. Peterson, S. C. Pieper, G. Savard, J. P. Schiffer, R. E. Segel, S. Sinha, X. Tang, and R. B. Wiringa, Search for excited states in  $^7\text{He}$  with the ( $d$ ,  $p$ ) reaction, *Phys. Rev. C* **72**, 061301(R) (2005).
- [7] N. Ryezayeva, C. Bäumer, A. Berg, L. Chulkov, D. Frekers, D. Frenne, E.-W. Grewe, P. Haefner, E. Jacobs, H. Johanson, Y. Kalmykov, A. Negret, P. Von Neumann-Cosel, L. Popescu, S. Rakers, A. Richter, G. Schrieder, A. Shevchenko, H. Simon, and H. Wörtche, Search for a low-energy resonance in  $^7\text{He}$  with the  $^7\text{Li}(d, ^2\text{He})$  reaction, *Phys. Lett. B* **639**, 623 (2006).
- [8] F. Skaza, V. Lapoux, N. Keeley, N. Alamanos, E. C. Pollacco, F. Auger, A. Drouart, A. Gillibert, D. Beaumel, E. Becheva, Y. Blumenfeld, F. Delaunay, L. Giot, K. W. Kemper, L. Nalpas, A. Obertelli, A. Pakou, R. Raabe, P. Roussel-Chomaz, J.-L. Sida *et al.*, Experimental evidence for subshell closure in  $^8\text{He}$  and indication of a resonant state in  $^7\text{He}$  below 1 MeV, *Phys. Rev. C* **73**, 044301 (2006).
- [9] A. H. Wuosmaa, J. P. Schiffer, K. E. Rehm, J. P. Greene, D. J. Henderson, R. V. F. Janssens, C. L. Jiang, L. Jisonna, J. C. Lighthall, S. T. Marley, E. F. Moore, R. C. Pardo, N. Patel, M. Paul, D. Peterson, S. C. Pieper, G. Savard, R. E. Segel, R. H. Siemssen, X. D. Tang *et al.*, Structure of  $^7\text{He}$  by proton removal from  $^8\text{Li}$  with the ( $d$ ,  $^3\text{He}$ ) reaction, *Phys. Rev. C* **78**, 041302(R) (2008).
- [10] A. Fomichev, L. Grigorenko, S. Krupko, S. Stepantsov, and G. Ter-Akopian, The ACCULINNA-2 project: The physics case and technical challenges, *Eur. Phys. J. A* **54**, 97 (2018).
- [11] A. A. Bezbakh, M. S. Golovkov, A. S. Denikin, R. Wolski, S. G. Belogurov, D. Biare, V. Chudoba, A. S. Fomichev, E. M. Gazeeva, A. V. Gorshkov, G. Kaminski, B. R. Khamidullin, M. Khirk, S. A. Krupko, B. Mauey, I. A. Muzalevskii, W. Piatek, A. M. Quynh, S. I. Sidorchuk, R. S. Slepnev *et al.*, Properties of the  $^7\text{He}$  ground state studied by the  $^6\text{He}(d, p)^7\text{He}$  reaction, *Int. J. Mod. Phys. E* **33**, 2450002 (2023).
- [12] A. Bezbakh, S. Belogurov, R. Wolski, E. Gazeeva, M. Golovkov, A. Gorshkov, G. Kaminski, M. Kozlov, S. Krupko, I. Muzalevskii, E. Nikolskii, E. Ovcharenko, R. Slepnev, G. Ter-Akopian, A. Fomichev, V. Chudoba, P. Sharov, and V. Schetin, A neutron spectrometer for experiments with radioactive beams on the ACCULINNA-2 fragment separator, *Instrum. Exp. Tech.* **61**, 631 (2018).
- [13] S. Agostinelli, J. Allison, K. Amako, J. Apostolakis, H. Araujo, P. Arce, M. Asai, D. Axen, S. Banerjee, G. Barrand, F. Behner, L. Bellagamba, J. Boudreau, L. Broglio, A. Brunengo, H. Burkhardt, S. Chauvie, J. Chuma, R. Chytracsek, G. Cooperman *et al.*, GEANT4—a simulation toolkit, *Nucl. Instrum. Methods Phys. Res. Sect. A* **506**, 250 (2003).
- [14] R. Lipperheide, Stripping into the continuum, *Phys. Lett. B* **32**, 555 (1970).
- [15] H. Fuchs, H. Homeyer, H. Oeschler, R. Lipperheide, and K. Möhring, Study of the off-energy-shell  $n$ - $^{15}\text{N}$  total cross section by means of  $^{15}\text{N}(d, p)$  stripping into the continuum of  $^{16}\text{N}$ , *Nucl. Phys. A* **196**, 286 (1972).
- [16] R. Lipperheide and K. Möhring, The reaction  $^{15}\text{N}(d, p)^{16}\text{N}(\text{unbound})$  and the off-energy-shell  $n$ - $^{15}\text{N}$  total cross section, *Phys. Lett. B* **39**, 323 (1972).
- [17] R. E. Azuma, E. Uberseder, E. C. Simpson, C. R. Brune, H. Costantini, R. J. de Boer, J. Görres, M. Heil, P. J. LeBlanc, C. Ugalde, and M. Wiescher, Azure: An  $R$ -matrix code for nuclear astrophysics, *Phys. Rev. C* **81**, 045805 (2010).
- [18] Z. Cao, Y. Ye, J. Xiao, L. Lv, D. Jiang, T. Zheng, H. Hua, Z. Li, X. Li, Y. Ge, J. Lou, R. Qiao, Q. Li, H. You, R. Chen, D. Pang, H. Sakurai, H. Otsu, M. Nishimura, S. Sakaguchi *et al.*, Recoil proton tagged knockout reaction for  $^8\text{He}$ , *Phys. Lett. B* **707**, 46 (2012).
- [19] S. Huang, Z. Yang, F. Marqués, N. Achouri, D. Ahn, T. Aumann, H. Baba, D. Beaumel, M. Boehmer, K. Boretzky, M. Caamaño, S. Chen, N. Chiga, M. Cortes, D. Cortina-Gil, P. Doornenbal, C. Douma, F. Dufter, J. Feng, and J. Zenihiro, Experimental study of  $4n$  by directly detecting the decay neutrons, *Few-Body. Syst.* **62**, 102 (2021).
- [20] S. Baroni, P. Navrátil, and S. Quaglioni, Unified *ab initio* approach to bound and unbound states: No-core shell model with continuum and its application to  $^7\text{He}$ , *Phys. Rev. C* **87**, 034326 (2013).
- [21] Y. Jaganathan, R. M. Id. Betan, N. Michel, W. Nazarewicz, and M. Płoszajczak, Quantified Gamow shell model interaction for *psd*-shell nuclei, *Phys. Rev. C* **96**, 054316 (2017).
- [22] I. A. Mazur, I. J. Shin, Y. Kim, A. I. Mazur, A. M. Shirokov, P. Maris, and J. P. Vary, SS-HORSE extension of the no-core shell model: Application to resonances in  $^7\text{He}$ , *Phys. Rev. C* **106**, 064320 (2022).
- [23] D. M. Rodkin and Y. M. Tchuvil'sky, Detailed theoretical study of the decay properties of states in the  $^7\text{He}$  nucleus within an *ab initio* approach, *Phys. Rev. C* **104**, 044323 (2021).